Supplementary Information

Design of humidity-resistant triboelectric nanogenerator based on CAU-10-$(SO_3H)_{0.08}(OH)_{0.92}$/PVC composites for producing hydrogen by water electrolysis application

Junhui Wu [a,b], *Baoping Yang* [a,*], *Jiahao Zhou* [b], *Yuan Ye* [b], *Ming Zhong* [b], *Yong Ding* [d], *Kun Zhao* [b,c,*]

[a] School of Petrochemical Technology, Lanzhou University of Technology, Lanzhou, Gansu, 730050, China

[b] State Key Laboratory of Advanced Processing and Recycling of Non-ferrous Metals, Lanzhou University of Technology, Lanzhou, Gansu, 730050, China

[c] Department of Chemistry, Tsinghua University, Beijing 100084, China

[d] School of Engineering, Qinghai Institute of Technology, Xining, Qinghai, 810016, China

*E-mail: zhaokun@lut.edu.cn, yangbaoping2004@163.com

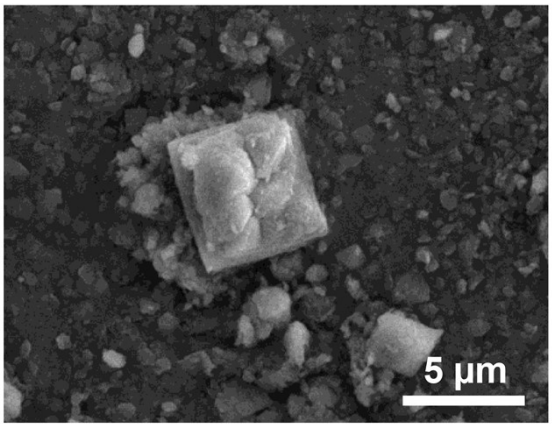

Fig. S1 SEM image of the prepared CAU-10-$(SO_3H)_{0.08}(OH)_{0.92}$ particles at magnifications of 3,000x.

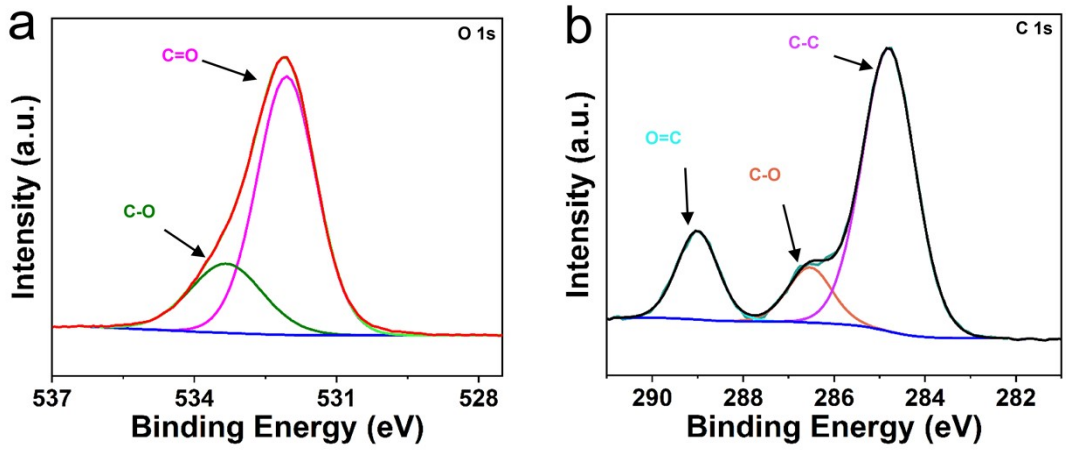

Fig. S2 High-resolution O 1*s* (a) and C 1*s* (b) XPS spectra of the prepared CAU-10-$(SO_3H)_{0.08}(OH)_{0.92}$ particles.

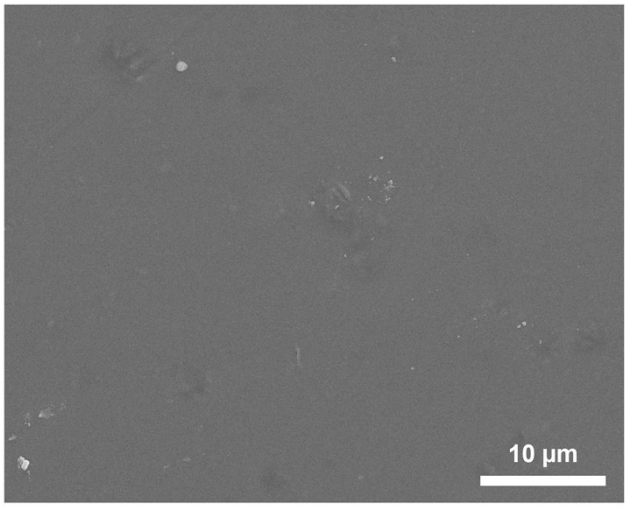

Fig. S3 SEM image of the CAU-10- $(SO_3H)_{0.08}(OH)_{0.92}$/PVC composite film.

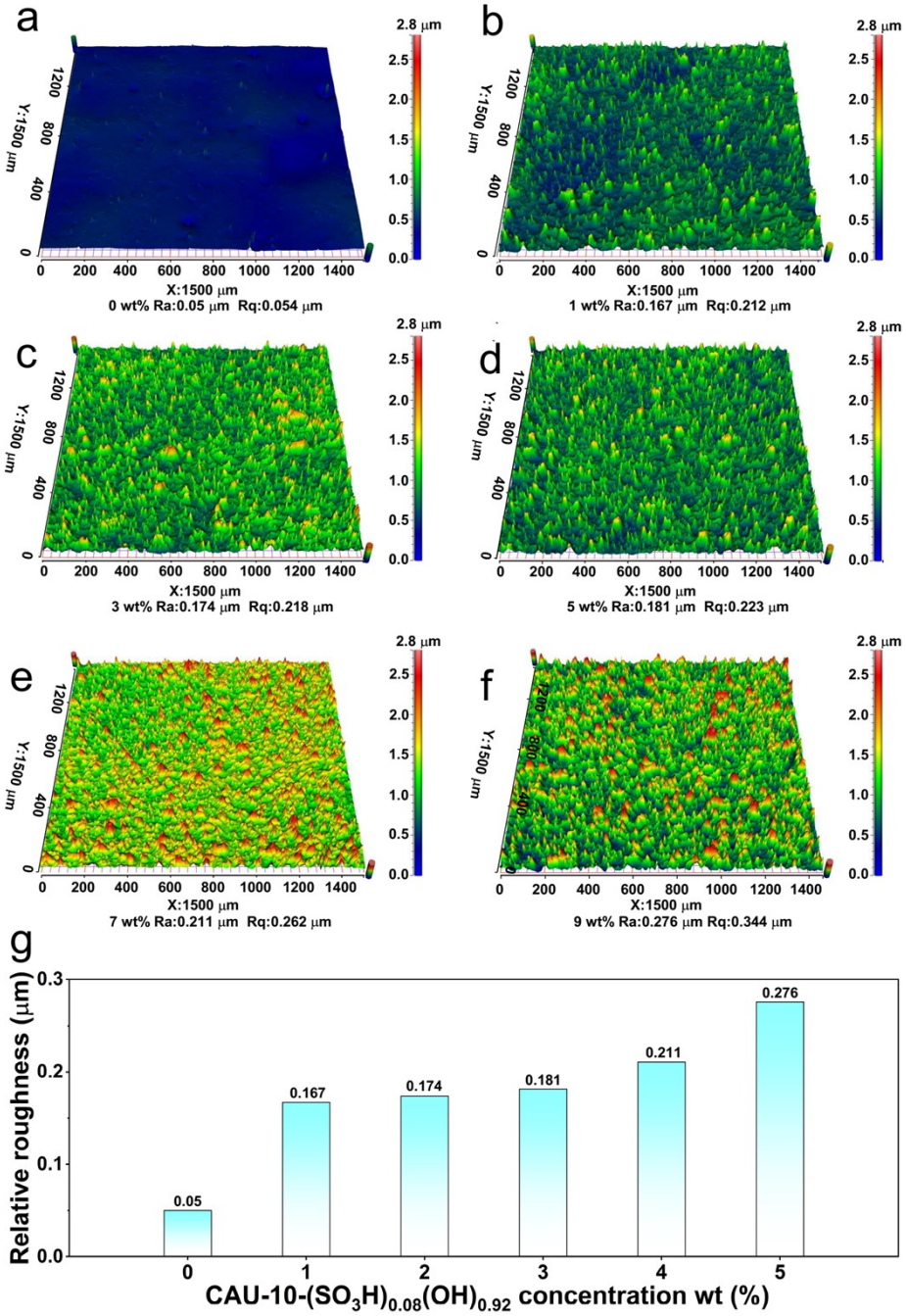

Fig. S4 (a-f) 3D surface morphologies of the CAU-10- $(SO_3H)_{0.08}(OH)_{0.92}$/PVC composite films at CAU-10- $(SO_3H)_{0.08}(OH)_{0.92}$ concentrations of 0 (a), 1 (b), 3 (c), 5 (d), 7 (e) and 9 wt% (f). **(g)** Histogram of surface relative roughness of CAU-10-$(SO_3H)_{0.08}(OH)_{0.92}$/PVC composite films at different CAU-10- $(SO_3H)_{0.08}(OH)_{0.92}$ concentrations.

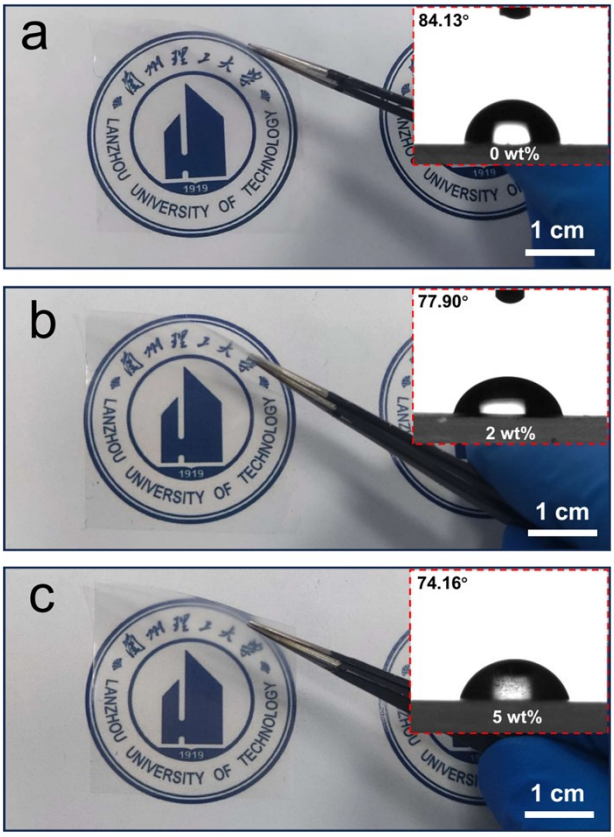

Fig. S5 Physical photographs of composite films under CAU-10-$(SO_3H)_{0.08}(OH)_{0.92}$ concentration of 0 (a), 2 (b) and 5 wt% (c), the insets are corresponding images of water droplets on the films.

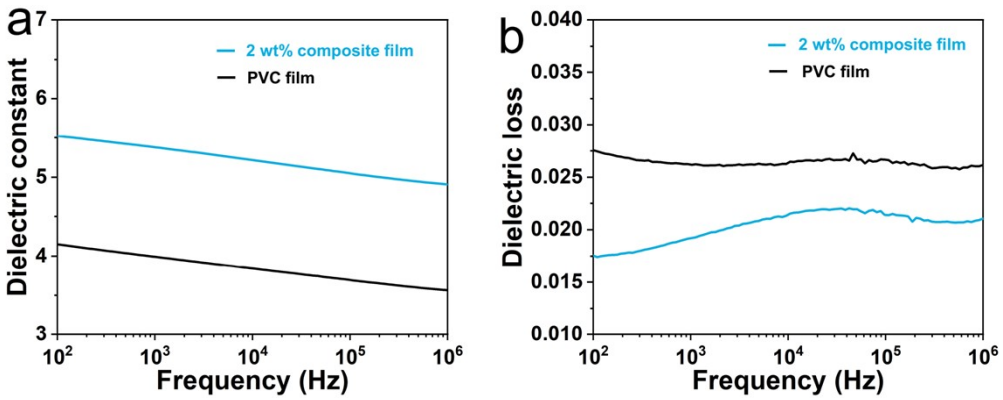

Fig. S6 Dielectric constant (a) and dielectric loss (b) of pure PVC film and 2 wt% CAU-10-$(SO_3H)_{0.08}(OH)_{0.92}$/PVC composite film.

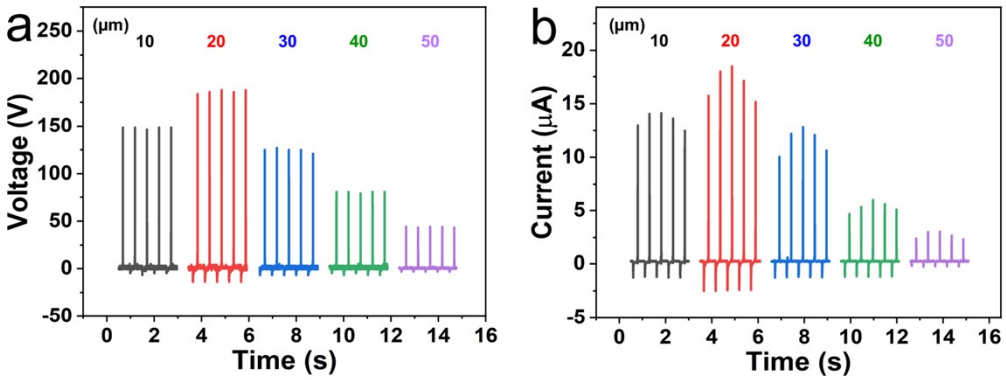

Fig. S7 Measured V_{oc} (a) and I_{sc} (b) of the TENG at different thickness of pure PVC films.

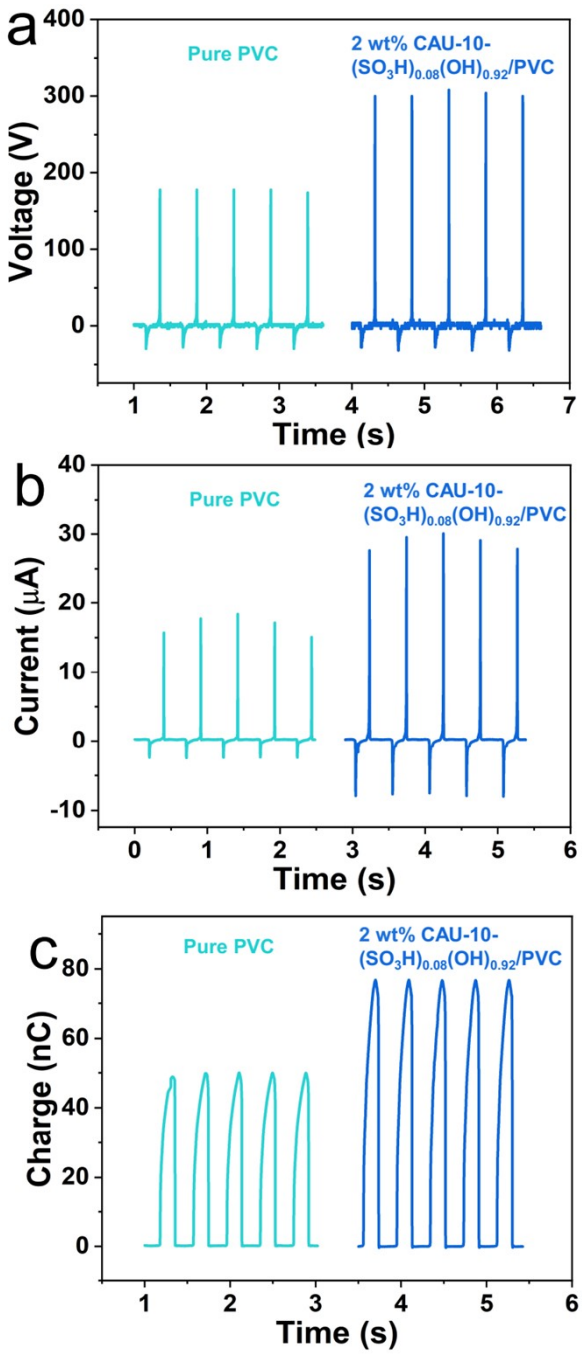

Fig. S8 Comparison of the measured V_{oc} (a), I_{sc} (b) and Q_{sc} (c) signals of the pure PVC-based TENG and the 2 wt% CAU-10-$(SO_3H)_{0.08}(OH)_{0.92}$/PVC-based TENG.

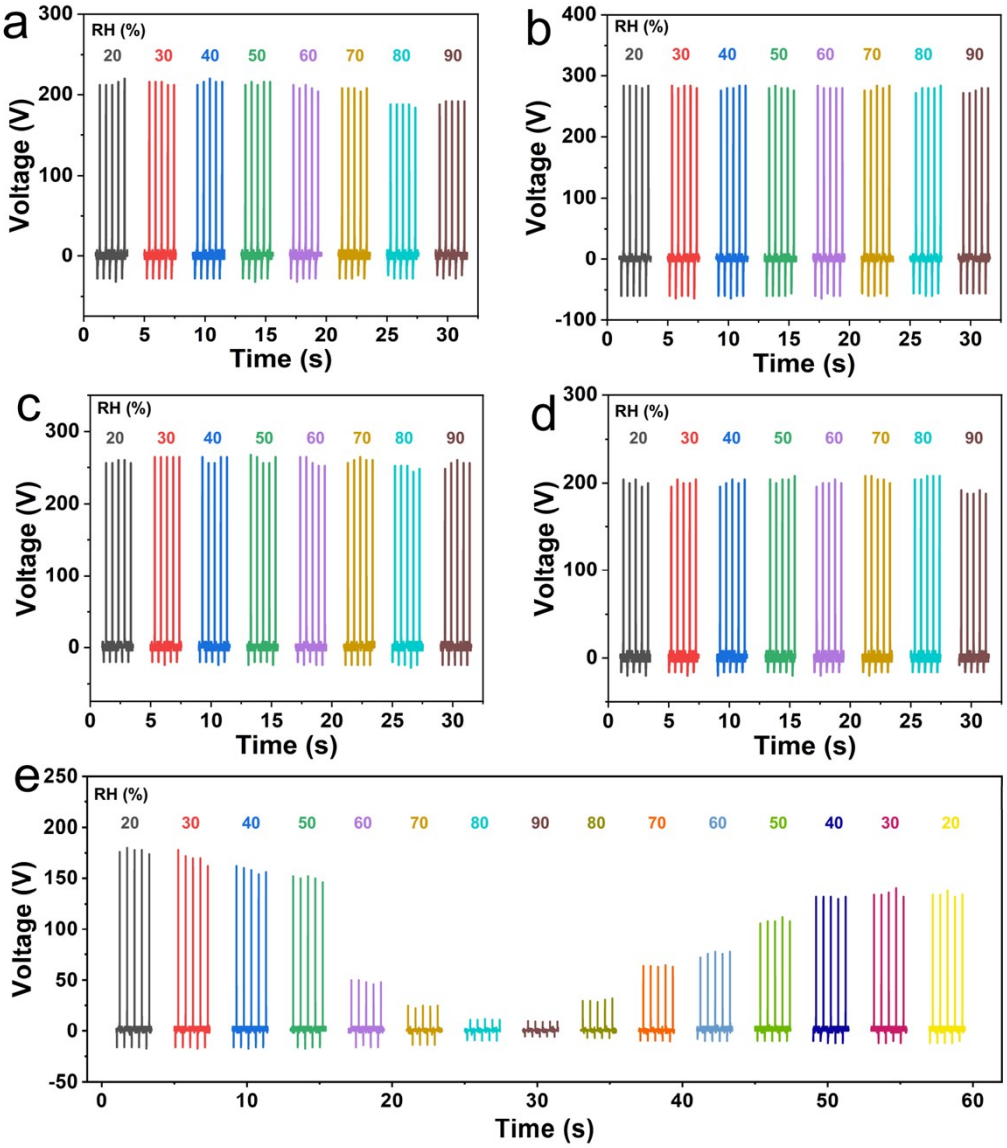

Fig. S9 (a-d) Measured V_{oc} signals of the TENG based on composite films with CAU-10-$(SO_3H)_{0.08}(OH)_{0.92}$ concentrations of 1 (a), 3 (b), 4 (c), and 5 wt% (d) at varying RH levels. (e) Measured V_{oc} signals of the pure PVC film-based TENG when RH first increases and then decreases.

Table S1 Comparison of output performance in MOF-based moisture-resistant TENGs.

Triboelectric materials	Size (cm)	Voltage/ Current	20-80 RH% voltage variation	Lifetime/ cycles	Ref.
CAU-10-$(SO_3H)_{0.08}(OH)_{0.92}$-PVC composite film and Al foil	6 × 6	318 V/ 30 μA	stable	36,000	This work
MOF-525/MXene/ Ecoflex composite film and latex gloves	3 × 3	2080 V/ 126 μA	decrease ~11.3 %	20,000	30
ZIF-8-PAN (ZIF-67-PAN) composite film and PAN	2 × 2	100 V/ 1.3 μA	decrease ~72.2 %	15,000	55
ZIF8/ZIF67 composite film and Teflon	2.5 × 2.5	359 V/ 11.7 μA	decrease ~69.1 %	10,080	56
Co-NPC/PVDF composite film and nylon-11	2.5 × 2.5	710 V/ 131.9 μA	decrease ~23.9 %	60,000	57

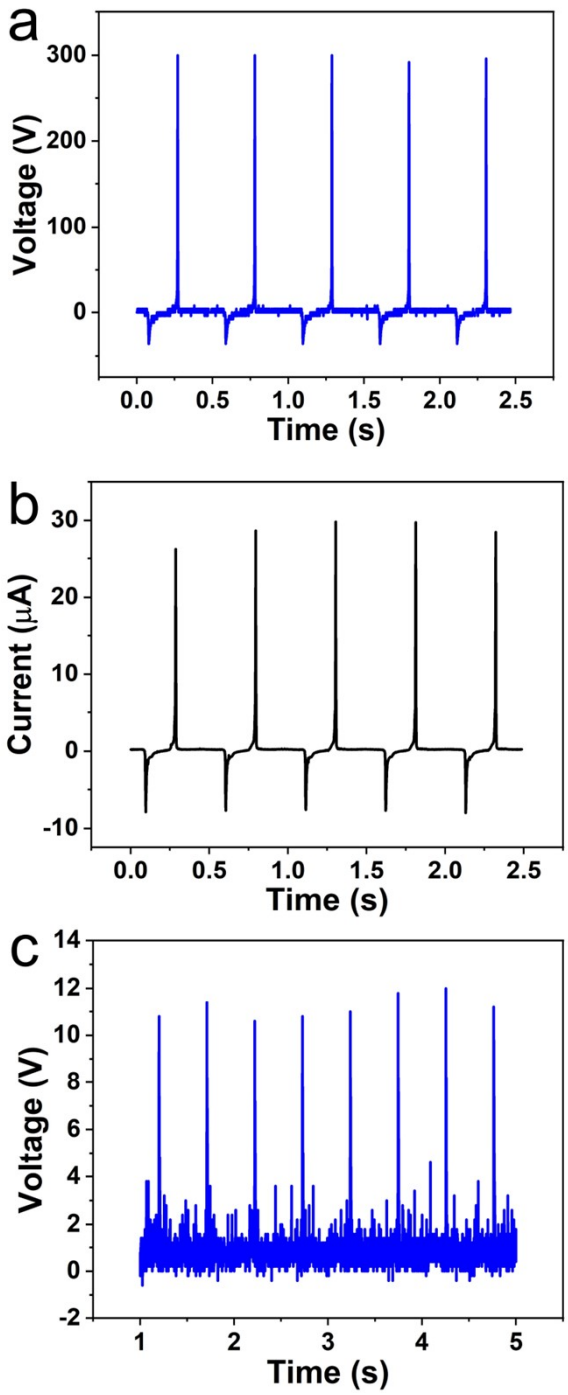

Fig. S10 (a,b) Measured V_{oc} (a) and I_{sc} (b) signals of the 2 wt% CAU-10-$(SO_3H)_{0.08}(OH)_{0.92}$/PVC film-based TENG without a transformer and a rectifier. (c) Measured V_{oc} signals of the 2 wt% CAU-10-$(SO_3H)_{0.08}(OH)_{0.92}$/PVC film-based TENG with a transformer and a rectifier.

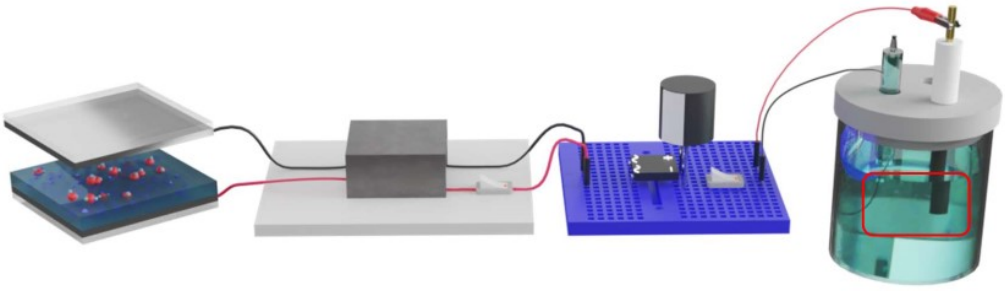

Fig. S11 (a) Schematic diagram of water electrolysis system based on the TENG.

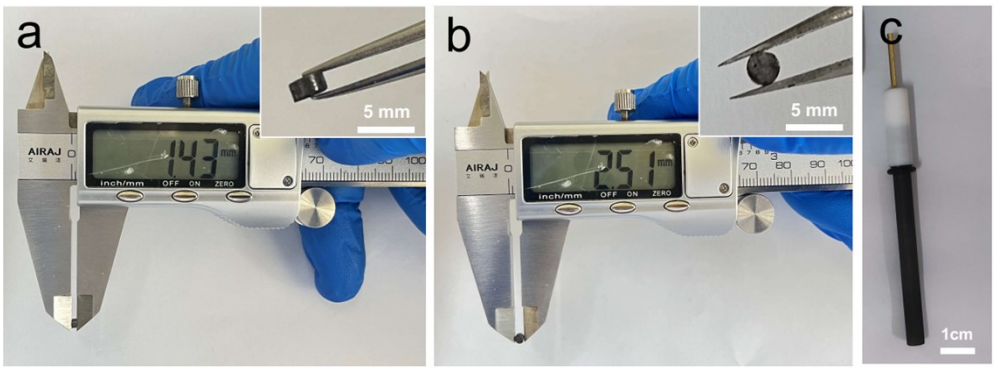

Fig. S12 Photographs of the height (a) and diameter (b) of carbon rod cathode. The corresponding insets are enlarged photos. (c) Photograph of graphite electrode.

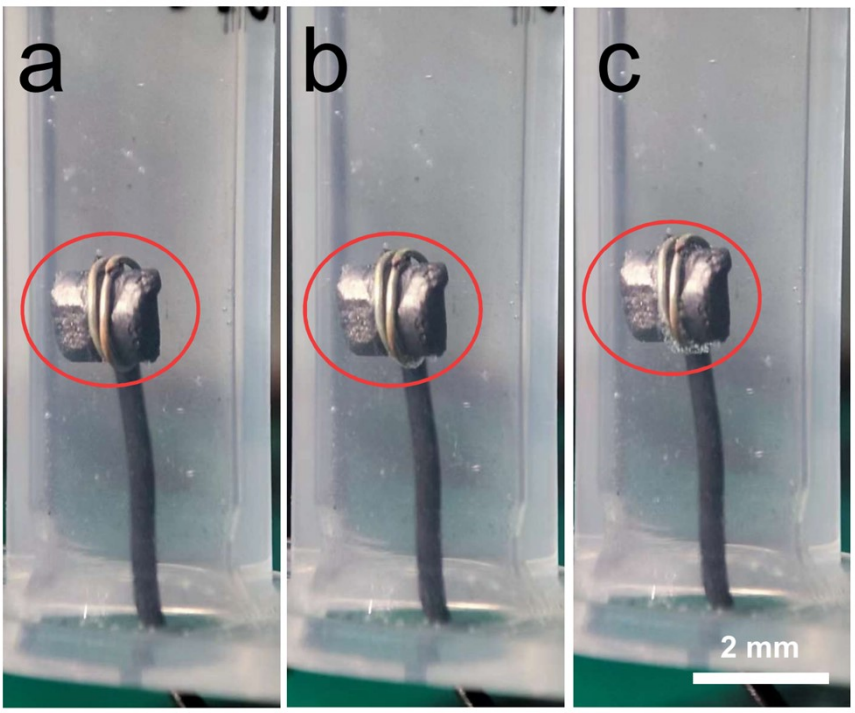

Fig. S13. Photographs of the bubbles produced on the cathode surface during the electrolysis of water with a charged capacitor at voltages of 2.3 (a), 2.5 (b) and 2.7 V (c).